

Article

Understanding the Sources of Ambient Fine Particulate Matter (PM_{2.5}) in Jeddah, Saudi Arabia

Shedrack R. Nayebare^{1,2}, Omar S. Aburizaiza³, Azhar Siddique³, Mirza M. Hussain^{1,2}, Jahan Zeb⁴, Fida Khatib², David O. Carpenter^{1,5} , Donald R. Blake⁶ and Haider A. Khwaja^{1,2,*}

¹ Department of Environmental Health Sciences, School of Public Health, University at Albany, Albany, NY 12201, USA; shedrack.nayebare@usp.org (S.R.N.); mirza.hussain@health.ny.gov (M.M.H.); dcarpenter@albany.edu (D.O.C.)

² Wadsworth Center, New York State Department of Health, Albany, NY 12201, USA; fida.khatib@health.ny.gov

³ Unit for Ain Zubaida Rehabilitation and Ground Water Research, King Abdul-Aziz University, P.O. Box 80200, Jeddah 21589, Saudi Arabia; orzizah@kau.edu.sa (O.S.A.); azsiddique@hubku.edu.qa (A.S.)

⁴ Department of Environmental and Health Research, The Custodian of the Holy Two Mosques Institute for Hajj and Umrah Research, Umm Al-Qura University, P.O. Box 6287, Makkah al Mukarramah 21955, Saudi Arabia; jzhabib@uqu.edu.sa

⁵ Institute for the Health & the Environment, University at Albany, Rensselaer, NY 12144, USA

⁶ Department of Chemistry, University of California, Irvine, CA 92617, USA; drblake@uci.edu

* Correspondence: haider.khwaja@health.ny.gov or hkhwaja@albany.edu; Tel.: +1-518-474-0516

Abstract: Urban air pollution is rapidly becoming a major environmental problem of public concern in several developing countries of the world. Jeddah, the second-largest city in Saudi Arabia, is subject to high air pollution that has severe implications for the health of the exposed population. Fine particulate matter (PM_{2.5}) samples were collected for 24 h daily, during a 1-year campaign from 2013 to 2014. This study presents a detailed investigation of PM_{2.5} mass, chemical composition, and sources covering all four seasons of the year. Samples were analyzed for black carbon (BC), trace elements (TEs), and water-soluble ionic species (IS). The chemical compositions were statistically examined, and the temporal and seasonal patterns were characterized using descriptive analysis, correlation matrices, and elemental enrichment factor (EF). Source apportionment and source locations were performed on PM_{2.5} samples using the positive matrix factorization (PMF) model, elemental enrichment factor, and air-mass back trajectory analysis. The 24-h mean PM_{2.5} and BC concentrations ranged from 33.9 ± 9.1–58.8 ± 25 µg/m³ and 1.8 ± 0.4–2.4 ± 0.6 µg/m³, respectively. Atmospheric PM_{2.5} concentrations were well above the 24-h WHO guideline of 15 µg/m³, with overall results showing significant temporal and seasonal variability. EF defined two broad categories of TEs: anthropogenic (Ni, V, Cu, Zn, Cl, Pb, S, Lu, and Br), and earth-crust derived (Al, Si, Mg, K, Ca, Ti, Cr, Mn, Fe, and Sr). The five identified factors resulting from PMF were (1) fossil-fuels/oil combustion (45.3%), (2) vehicular emissions (19.1%), (3) soil/dust resuspension (15.6%), (4) industrial mixed dust (13.5%), and (5) sea-spray (6.5%). This study highlights the importance of focusing control strategies, not only on reducing PM concentration but also on the reduction of components of the PM as well, to effectively protect human health and the environment.

Keywords: PM_{2.5}; black carbon; enrichment factor; PMF; mass reconstruction; Jeddah



Citation: Nayebare, S.R.; Aburizaiza, O.S.; Siddique, A.; Hussain, M.M.; Zeb, J.; Khatib, F.; Carpenter, D.O.; Blake, D.R.; Khwaja, H.A.

Understanding the Sources of Ambient Fine Particulate Matter (PM_{2.5}) in Jeddah, Saudi Arabia. *Atmosphere* **2022**, *13*, 711. <https://doi.org/10.3390/atmos13050711>

Academic Editor: Sunling Gong

Received: 30 March 2022

Accepted: 27 April 2022

Published: 29 April 2022

Publisher's Note: MDPI stays neutral with regard to jurisdictional claims in published maps and institutional affiliations.



Copyright: © 2022 by the authors. Licensee MDPI, Basel, Switzerland. This article is an open access article distributed under the terms and conditions of the Creative Commons Attribution (CC BY) license (<https://creativecommons.org/licenses/by/4.0/>).

1. Introduction

Fine particulate (PM_{2.5}) air pollution remains a major issue in Saudi Arabia, attributed largely to heavy industrialization and urbanization [1,2], with no proper policy implementation in place. This has progressively led to poor urban air quality. Over time, the number of both stationary (oil refineries, petrochemical industries, desalinization plants, power generation, etc.), and mobile sources (heavy trucks, buses, cars, etc.) of air pollution have increased tremendously. There was an estimated >1.4 million cars in Jeddah in 2012 [3]. This

number has most likely increased over the years. Fine particulate (PM_{2.5}) emissions from these sources significantly affect air quality.

Indeed, a few studies [1–4] assessing PM_{2.5} air pollution in Saudi Arabia's major cities reported poor air quality, mainly linked to industrial and vehicular emissions. Overall, there is a major consensus that anthropogenic sources contribute significantly to the observed air pollution in Saudi Arabia. The World Health Organization (WHO) recommends annual, and 24-h mean PM_{2.5} at 5 and 15 µg/m³, respectively [5]; and the Presidency of Meteorology and Environment (PME) of Saudi Arabia regulates PM_{2.5} at 15 and 35 µg/m³ annual and 24-h mean, respectively [6]. Most of the studies done in Saudi Arabia's major cities [1,2,7,8] showed evidence of PM_{2.5} levels exceeding both the PME and WHO guidelines, as well as the levels recorded in Europe [9–12] and North America [13–16].

In addition, mounting evidence from several epidemiologic studies has shown that exposure to fine particulate air pollution, at much lower levels than reported in this study, significantly increases the risk of morbidity and mortality from cardiopulmonary diseases [17–20], and exacerbates pre-existing medical conditions such as asthma, coronary obstructive pulmonary disease [21,22], and other illnesses, notably among children and the elderly. Given the extent of the adverse health outcomes reported at much lower PM_{2.5} levels, this further accentuates the need for more studies assessing air quality in Saudi Arabia and the rest of the Middle East. This study becomes one of the pioneer studies to fully characterize the state of air quality in Jeddah, providing a breakdown on the major emission sources.

The chemical and physical characterization of PM_{2.5} is key to understanding its toxicity, as well as elucidating more on the possible emission sources. This is critical to the design and implementation of more effective policies, and ultimately, the preservation of human health and the environment. For Jeddah, being one of the major industrialized cities in Saudi Arabia, results from this study will be fundamental to the improvement of existing local and regional policies on air pollution, mainly targeting the major anthropogenic sources. This study addresses four main objectives: (1) providing a detailed assessment of the levels of ambient PM_{2.5}, black carbon (BC), trace elements, and water-soluble ionic species; (2) discussion of the temporal and seasonal variabilities in air pollution levels and composition; (3) source apportionment using factor analysis approaches (elemental enrichment factor and positive matrix factorization); and (4) discussion of some of the suggested recommendations for current and future air pollution control in Jeddah and other cities in the region.

2. Materials and Methods

2.1. Study Area

Jeddah city (Figure 1) is the second-largest city in Saudi Arabia, located in the Hijaz Tihamah region (Lat. 21.3° North and Lon. 39.2° East), midway eastern shore of the Red Sea. The city has a municipality area of 5460 km² and population of 3.98 million people [23]. Jeddah features a semi-arid to arid climate [24]. Rainfall only occurs around November to January, with an annual mean of 44.6 mm (<http://www.holiday-weather.com/jeddah/averages/> accessed on 4 May 2021). The city is characterized by heavily industrialized areas with different types of industries (such as oil refineries, desalination, iron smelting, etc.), heavy vehicular traffic, and sandstorms.

Due to its location, Jeddah's prevailing winds are frequently northwesterly. During winter, spring, and fall, blustery winds also blow from the south, causing sandstorms, sometimes accompanied by thunderstorms and heavy rains [24]. Winters are warm, from 15–18 °C at dawn to ≥28 °C in the afternoon. Summers are hot and humid (≥40 °C in the afternoon and ≥31 °C in the evening). These weather conditions directly influence the levels of PM_{2.5}. More climate information on Jeddah can be found at: <http://www.jeddah.climateps.com/> (accessed on 4 May 2021).

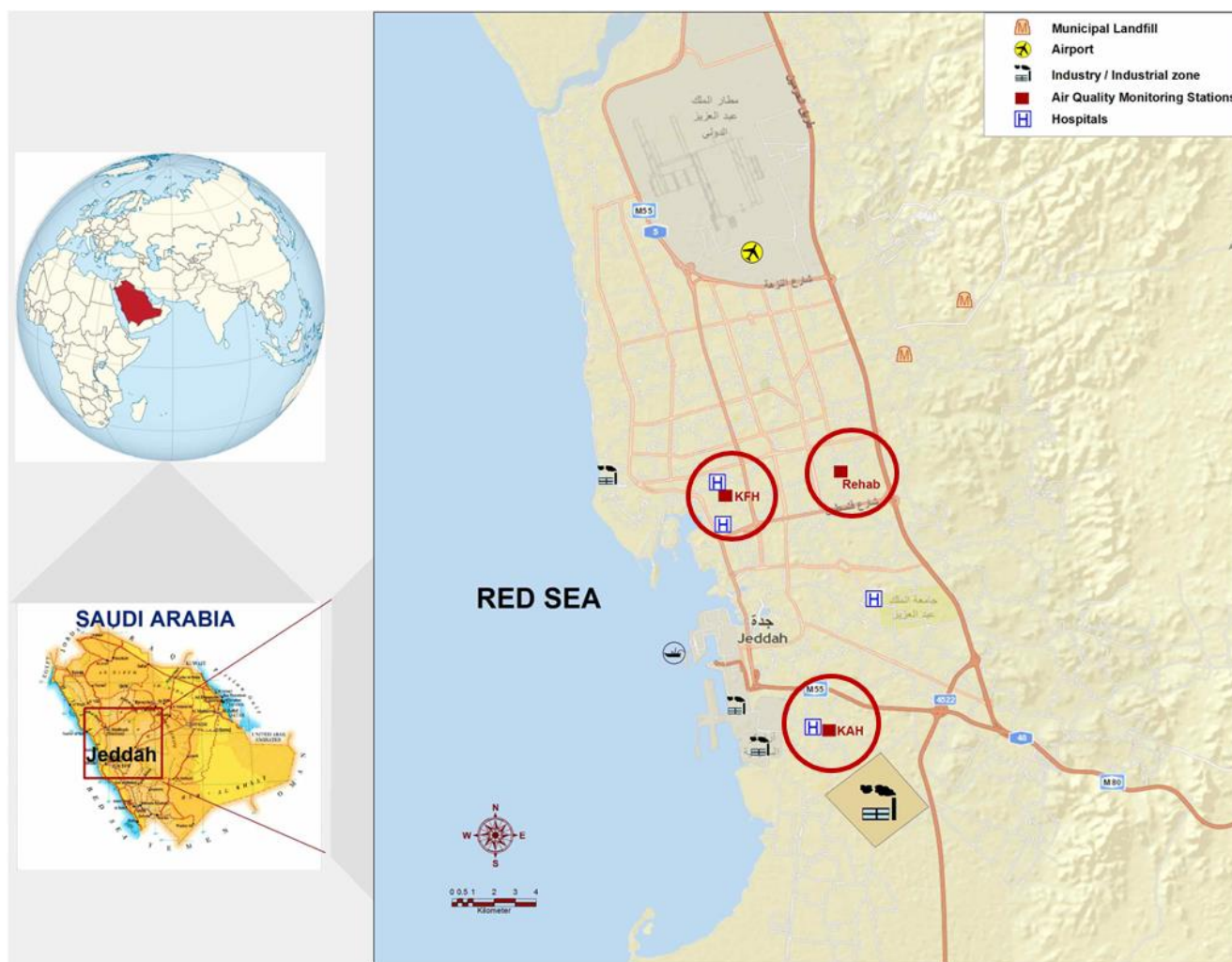


Figure 1. Map of Jeddah showing the sampling sites (King Abdul-Aziz Hospital (KAH), King Fahad Hospital (KFH), King Abdul-Aziz University (Al-Rehab/KAU)), industrial areas, major roads, and hospitals. Al-Rawda sampling site not depicted.

2.2. $PM_{2.5}$ Sampling and Analysis

$PM_{2.5}$ samplers were installed at three fixed sampling sites (Figure 1). Sampling was done for six weeks in each quarter of the year starting from 8 April 2013–18 February 2014. Each quarter represented a sampling cycle. The first and second cycles were sampled at King Abdul-Aziz Hospital (KAH) and King Fahad Hospital (KFH), while the third and fourth were at KAH and Al-Rehab/or KAU (King Abdul-Aziz University) sites. The first 10 days of cycle 1 were sampled at Al-Rawda, and the rest at the KFH site. These sampling sites were selected in such a way as to represent a relatively uniform blend of residential and industrial areas. Residential sites were densely populated areas, while the heavy traffic and industrial areas represented industrial sites. This resulted in a representative mix for both the residential and industrial areas, and thus, a more accurate estimation of the actual pollution levels in real time. Meteorology data were obtained online from <https://www.wunderground.com> (accessed on 4 May 2021).

The 24-h $PM_{2.5}$ samples were collected on pre-weighed, sequentially labeled Whatman 46.2 mm diameter 2.0 μm pore polytetrafluoroethylene (PTFE) filters (Whatman plc, Florham Park, NJ, USA) using a low volume air sampling pump (VS23 series pump, HI-Q Environmental Products Company, Inc., San Diego, CA, USA). The $PM_{2.5}$ sampler (Figure S1) was equipped with a cyclone separator with a cut size of 2.5 μm operated at a flow rate 16.7 ± 0.84 L/min, optimum for sampling the $PM_{2.5}$ size range. The sampler

inlets were fixed at about 5 m above the ground for a good representation of ambient PM_{2.5} and to avoid influence of ground dust. The sampled filters were stored in labeled clean polypropylene petri-dishes and immediately refrigerated at 4 °C to minimize further loss of temperature sensitive ammonium, nitrate, and oxalate. At the end of the sampling cycle, all the samples were shipped to the Wadsworth Center, New York State Department of Health, Albany, NY, USA, to be analyzed for PM_{2.5} levels, black carbon (BC), trace elements (TEs), and water-soluble ionic species. The samples were refrigerated until analysis. Given the large number of samples corrected, analysis for the different pollutants was completed within 3–4 months of receiving the samples.

The 24-h PM_{2.5} levels were determined gravimetrically as the difference of the PTFE filter weight before and after sampling. BC loading ($\mu\text{g}/\text{m}^3$) on the filters was determined using a dual-wavelength Optical Transmissometer (Model OT-21, 2007), Magee Scientific, Francisco St, Berkeley, CA, USA. The OT-21 collects absorbance data at 370 nm and 880 nm wavelengths. To correct for the loading effects, we applied attenuation coefficients $K_{880\text{nm}} = 16.6 \text{ m}^2 \text{ g}^{-1}$ and $K_{370\text{nm}} = 39.5 \text{ m}^2 \text{ g}^{-1}$ [25] at respective channels. The difference between $\text{BC}_{370\text{nm}}$ and $\text{BC}_{880\text{nm}}$ estimates $\Delta\text{-C}$ (Equation (1)), a marker for organic matter combustion [26,27].

$$\Delta\text{-C} = \text{BC}_{370\text{nm}} - \text{BC}_{880\text{nm}} \quad (1)$$

TEs were analyzed by an energy dispersive X-ray fluorescence (ED-XRF) spectrometer (Thermo Scientific™, Waltham, MA, USA) using six secondary fluorescers (Si, Ti, Fe, Cd, Se, and Pb). ED-XRF has been extensively used for TEs analysis in air particulate samples [28–30] because it is fast and does not require chemical digestion of samples prior to analysis [31], which minimizes contamination. This technique works on a principle that distinct atoms, when excited by an external high energy, will emit X-ray photons with characteristic energy and wavelengths. So, TEs in a sample can be identified and quantified by measuring the intensity of photons of each energy emitted from the sample [32,33]. The intensity of radiation signal from each TE in the sample, which is also proportional to its concentration, is then computed from a set of internal calibration curves.

The water-soluble ionic species were analyzed using ion-exchange chromatography (IC) (Dionex, Sunnyvale, CA, USA). A summary of the optimized conditions used for the analysis of water-soluble ionic species by IC, has been included in the Supplemental Materials (Table S1). Strict quality control and quality assurance measures were taken throughout the study. Typical detection limits of trace elements measured in this study are provided in Supplemental Materials (Table S2, based on [34]). More details of the sampling and analyses for PM_{2.5} levels, BC, TEs, and ionic species have been previously provided [1,7].

2.3. PM_{2.5} Mass-Reconstruction

We performed PM_{2.5} mass-reconstruction by re-grouping the chemical species measured in PM_{2.5} aerosol into six major categories [1]: (1) crustal/geological materials; (2) anthropogenic trace elements (TEs); (3) secondary inorganic ions (IS) (SO_4^{2-} , NO_3^- , NH_4^+ , and $\text{C}_2\text{O}_4^{2-}$); (4) sea salt/sea sprays; (5) black carbon (BC)/soot; and (6) particulate organic matter (POM). These categories makeup the proportion of the overall PM_{2.5} explained by the measured pollutant species in our analyses [35]. Additional details on the frequently applied mass-reconstruction equations and the backgrounds and assumptions related to each pollutant category can be found in several previous studies [35,36]. The reconstructed PM_{2.5} mass was calculated as shown in Equation (2):

$$\text{Reconstructed PM}_{2.5} = \text{Crustal Material [CM]} + \text{Trace Elements [TE]} + \text{Sea Spray [SS]} + \text{Secondary Ions [SI]} + \text{Elemental Carbon [EC/ or BC]} + \text{Organic Matter [OM]} \quad (2)$$

where:

$$[\text{CM}] = 1.89[\text{Al}] + 1.21[\text{K}] + 1.43[\text{Fe}] + 1.4[\text{Ca}] + 1.66[\text{Mg}] + 1.67[\text{Ti}] + 2.14[\text{Si}] \quad (3)$$

$$[\text{TE}] = 1.31[\text{V}] + 1.46[\text{Cr}] + 1.29[\text{Mn}] + 1.27[\text{Ni}] + 1.13[\text{Cu}] + 1.24[\text{Zn}] + 1.32[\text{As}] + 1.41[\text{Se}] + 1.40[\text{Br}] + 1.37[\text{Sr}] + 1.14[\text{Er}] + 1.12[\text{Ba}] + 1.14[\text{Lu}] + 1.08[\text{Pb}] \quad (4) \text{ [7,37,38]}$$

$$[\text{SS}] = [\text{Cl}^-] + \text{ss} [\text{Na}^+] + \text{ss} [\text{Mg}^{2+}] + \text{ss} [\text{K}^+] + \text{ss} [\text{Ca}^{2+}] + \text{ss} [\text{SO}_4^{2-}] \quad (5)$$

where $\text{ss} [\text{Na}^+] = 0.556 [\text{Cl}^-]$; $\text{ss} [\text{Mg}^{2+}] = 0.12 \text{ss} [\text{Na}^+]$; $\text{ss} [\text{K}^+] = 0.036 \text{ss} [\text{Na}^+]$; $\text{ss} [\text{Ca}^{2+}] = 0.038 \text{ss} [\text{Na}^+]$; and $\text{ss} [\text{SO}_4^{2-}] = 0.252 \text{ss} [\text{Na}^+]$ [39].

$$[\text{SI}] = \text{nss} [\text{SO}_4^{2-}] + [\text{NO}_3^-] + [\text{NH}_4^-] + [\text{C}_2\text{O}_4^{2-}] \quad (6)$$

where $\text{nss} [\text{SO}_4^{2-}] = [\text{SO}_4^{2-}] - \text{ss} [\text{SO}_4^{2-}]$; ss and nss denote sea spray and non-sea spray, respectively.

The oxide factors used in Equations (3) and (4) were estimated bases on the most stable oxides (Al_2O_3 , K_2O , Fe_2O_3 , CaO , MgO , TiO_2 , SiO_2 , VO , Cr_2O_3 , MnO , NiO , Cu_2O , ZnO , As_2O_3 , SeO_2 , BrO_2 , SrO_2 , Er_2O_3 , BaO , Lu_2O_3 , and PbO) of these elements [7,37,38].

2.4. $\text{PM}_{2.5}$ Source Apportionment

We performed source apportionment for $\text{PM}_{2.5}$ using three approaches; $\text{PM}_{2.5}$ mass-reconstruction, elemental enrichment factor (EF), and positive matrix factorization (PMF). Results were carefully studied from the three approaches to accurately define the sources of $\text{PM}_{2.5}$ in Jeddah.

Enrichment factors (EFs) were calculated using Al as a reference element (Equation (7)) to assess the extent of anthropogenic contributions to the measured $\text{PM}_{2.5}$ levels, as explained in previous studies and some of our past work [26,27].

$$\text{EF} = \frac{(C_x/C_{\text{Al}})_{\text{PM}_{2.5}}}{(C_x/C_{\text{Al}})_{\text{Earth-crust}}} \quad (7)$$

C_x and C_{Al} denote the levels of the element "x" and "Al", respectively, in the ambient $\text{PM}_{2.5}$ sample and the earth-crust. The relative abundances of trace elements in the earth-crust were obtained from Taylor (1964). EF values greater than 10 suggest a significant anthropogenic contribution, while EF values less than 10 are indicative of major contributions from the earth-crust. Generally, the EF values between 10 to 50 are indicative of mixture of anthropogenic and earth-crust derived emissions, while EF values greater than 50 are indicative of purely anthropogenic emissions.

To delineate various sources of $\text{PM}_{2.5}$, we used the latest the United States Environmental Protection Agency (U.S.EPA) positive matrix factorization (PMF) receptor model (version 5.0.14). This is a mathematical receptor model that utilizes a multivariate factor analysis to breakdown a complex matrix of well speciated sample data (containing both concentration and uncertainty estimates) into two simpler matrices as factor profiles and factor contributions. Based on the species within each profile, we drew interpretations for the source types using the measured chemical species in the samples as markers for specific sources. More details on PMF analysis and the resolution, interpretation of factors, and the QA/QC measures have been provided in several previous studies [40–42].

We utilized the backward-in-time hybrid single-particle Lagrangian integrated trajectories (HYSPLIT) set at an altitude of 500 m above sea level, to determine the direction of air-mass flow. The atmospheric boundary layer (ABL), which is the lowest part of the atmosphere, is about 50 to 3000 m above sea-level [43]. This is the space where most of the anthropogenic activities and meteorological trends occur. Obtaining an accurate estimate of the ABL for a given study area is of a critical importance in air pollution studies. Previously reported data show that the depth of the mixed layer over the Arabian Sea ranges from 400 to 900 m, but with high variability near the shores due to the intricate nature of the interactions between the land and sea breezes [44]. In another study, Jeddah's ABL was estimated around 900 m, but with some variability [45]. Given the range of ABL estimates around the Arabian Sean and Jeddah, we ran our HYSPLIT models set at 500 m above the sea level because this height provides a representative regional ABL where most

anthropogenic activities take place. However, most importantly, the significance of this ABL height is that; (1) it is optimum for long-range atmospheric transport of pollutants, and (2) it has a direct influence on human exposure risk. Pollutants dispersed over 500 m above sea-level will be transported over a much longer distance, but the possibility of human exposure is significantly diminished to almost zero. So, as we assessed the wind trajectories, our focus remained centered around the question of how this influences human exposure. Trajectories covering a period of up to 72 h prior to sampling date were computed to determine the direction of air mass flow into the study area. The plots for backward-in-time trajectories with their respective data files were downloaded from the National Oceanic and Atmospheric Administration (NOAA) website [46,47]. When interpreted correctly, wind trajectories can provide insightful information about the contribution of the regional and local emissions towards the observed levels of PM_{2.5}.

3. Results and Discussion

3.1. PM_{2.5} Mass and Chemical Composition

The mean daily (24-h) PM_{2.5} and its components (BC, TEs, and IS), and meteorology, are summarized in Table 1. The mean daily temperature was relatively stable (25.0–29.6 °C), while relative humidity (RH) and wind speed (WS) varied significantly throughout the study period (Figure 2). Additionally, the 24-h PM_{2.5} displayed significant temporal variability with the mean PM levels per cycle, far exceeding the 24-h WHO guideline (25 µg/m³), 91% of the study period (Figure 2). Overall, PM_{2.5} levels gradually increased around January and February (cycle 4) and was highest in April and May (cycle 1). This seasonal trend may partly be linked to meteorology. Jeddah experiences strong winds and sandstorms during winter and spring [48]. This may account for a significant portion of the high PM_{2.5} levels recorded during cycles 1 and 4. Moreover, the ambient temperature inversion during winter lowers the atmospheric boundary layer, which in turn limits the dispersion of airborne pollutants. Ultimately, this leads to increased concentration of ambient PM_{2.5} as observed in this study.

Black carbon (BC) had a significant daily variability but with no major seasonal variability observed (Figure 2). This was linked to BC being mostly associated with vehicular and industrial emissions. Emissions from these sources may fluctuate significantly by the day of the week (weekday–weekend trends), but not by season. BC, as represented by a signal at infra-red λ (BC_{IR}), explained only 3.6–7.2% of the total PM_{2.5}. In addition, the mean delta-C levels per cycle were below zero (Table 1). Only two (2) days in cycle 1 had delta-C > 0 (0.01 and 0.14 µg/m³). Delta-C, computed as the difference in BC measurements at ultraviolet λ (BC_{UV}) and BC_{IR}, is a strong marker for organic matter combustion [26,27]. Thus, the observed results in this study point to a minor or no contribution from biomass burning to the overall recorded PM_{2.5} levels in Jeddah.

Up to twenty-four (24) trace elements (TEs) were detected at levels above their respective limits of quantification (LOQ), as per the analytical method used (Table 1). Crustal elements (Si, Ca, Fe, Al, and Mg) recorded the highest concentrations, signaling a significant influence from the earth crust/soil. Sulfur (S), Cl, and Na also constituted the most abundant elements. Several anthropogenic TEs (S, Ni, V, Cu, Y, Zn, Cl, S, Pb, Br, Lu, and Ce) were detected. These TEs are intricately linked to vehicular emissions (Pb, Ni, Cu, Br, and Ce), fossil-fuels/oil combustion (S, V, and Lu), and other industrial processes [49,50].

The water-soluble ionic species (IS) were mostly sulfate (SO₄²⁻), nitrate (NO₃⁻), and ammonium (NH₄⁺), as shown in Table 1. High concentrations of SO₄²⁻ and NO₃⁻ species in the ambient air can be indicative of significant anthropogenic emissions from fossil-fuels/oil combustion (SO₄²⁻) and vehicular emissions (NO₃⁻).

Table 1. Summarized 24-h PM_{2.5}, BC, TEs, IS, and meteorology (mean daily temperature, relative humidity (RH) and wind speed (WS)) per sampling cycle in Jeddah.

Parameter	Cycle 1			Cycle 2			Cycle 3			Cycle 4		
	Mean ± S.D	Min	Max	Mean ± S.D	Min	Max	Mean ± S.D	Min	Max	Mean ± S.D	Min	Max
PM _{2.5} (µg/m ³)	58.8 ± 25	22.3	118	36.2 ± 12.3	21.3	80	33.9 ± 9.1	18.5	63	38 ± 17.7	12.4	90.8
BC _{IR} (µg/m ³)	1.9 ± 0.6	0.8	2.9	1.8 ± 0.4	0.8	2.7	2.4 ± 0.6	1.4	4.0	2.3 ± 0.8	0.9	4.6
BC _{UV} (µg/m ³)	1.6 ± 0.5	0.7	2.6	1.2 ± 0.3	0.6	1.8	1.6 ± 0.3	0.1	2.3	1.6 ± 0.5	0.7	3.3
Delta-C (µg/m ³)	−0.3 ± 0.2	−0.9	0.1	−0.6 ± 0.2	−1.02	−0.2	−0.8 ± 0.3	−1.7	−0.3	−0.6 ± 0.3	−1.3	−0.2
RH (%)	53.6 ± 8.1	38.0	71	56.2 ± 8.0	30.0	71	63.8 ± 6.8	47	78	51.9 ± 12	26	71.0
Temp. (°C)	29.6 ± 2.6	24.4	34.4	27.2 ± 0.8	31.1	35.6	29.6 ± 1.2	27.8	31.7	25 ± 1.8	20	27.8
WS (m/s)	6.5 ± 2.1	3.0	11	6.6 ± 1.5	4.0	10	5.4 ± 1.6	3.0	10	7.5 ± 3.0	3.0	15
Trace Elements, TEs (ng/m³)												
Sulfur (S)	4972 ± 2577	1323	10,935	4434 ± 1301	1271	7973	6838 ± 2714	2629	15,224	4348 ± 2216	1214	9549
Silicon (Si)	3427 ± 2076	727	12,733	2727 ± 3783	397	16,469	2255 ± 931	578	4197	3748 ± 2739	723	14,151
Calcium (Ca)	1780 ± 1404	660	10,015	1049 ± 565	455	2730	1216 ± 367	628	2037	1863 ± 1342	500	7380
Iron (Fe)	1367 ± 772	354	4760	1252 ± 1622	283	7295	945 ± 340	318	1665	1565 ± 1117	347	5549
Aluminum (Al)	1227 ± 832	177	5116	1052 ± 1662	53.1	7191	830 ± 361	152	1568	1193 ± 988	96.8	4812
Sodium (Na)	1065 ± 516	434	2919	1151 ± 721	172	2552	953 ± 456	480	2090	735 ± 388	237	1723
Chlorine (Cl)	547 ± 997	<DL	5621	261 ± 477	<DL	1674	108 ± 364	<DL	2150	219 ± 389	<DL	1882
Magnesium (Mg)	516 ± 232	227	1688	397 ± 234	169	1181	454 ± 121	241	767	439 ± 305	108	1663
Potassium (K)	490 ± 287	259	2160	412 ± 234	208	1236	412 ± 76.8	286	558	460 ± 292	153	1622
Lead (Pb)	318 ± 401	2.73	1783	89.2 ± 190	<DL	1157	294 ± 304	4.71	1142	361 ± 441	16.1	2298
Titanium (Ti)	126 ± 77.9	28.8	498	112 ± 146	25	628	85.3 ± 30	26.9	152	141 ± 94	30.2	458
Zinc (Zn)	90.5 ± 149	11.6	696	60.9 ± 94.6	9.7	494	52.1 ± 44.5	12.1	206	53.3 ± 49.9	12.1	224
Bromine (Br)	50.2 ± 14.8	24.5	92.5	64 ± 22.9	21.2	114	68.2 ± 18.4	36.5	130	51.4 ± 20.3	25.7	136
Vanadium (V)	36.5 ± 19.8	<DL	80.9	41.6 ± 14.2	22.1	74.7	32.8 ± 14.4	8.5	67.9	15.1 ± 13.1	<DL	50.4
Manganese (Mn)	31.3 ± 16.9	9.5	77.7	26.2 ± 32.4	3.4	144	22.6 ± 8.7	6.1	41.5	35.3 ± 28.9	7.7	148
Lutetium (Lu)	21.4 ± 15.5	5.0	71.5	16.7 ± 11.4	6.2	56.6	15.8 ± 7.4	3.5	35	18.5 ± 9.9	6.2	46
Nickel (Ni)	17.3 ± 8.8	3.9	40.3	17.1 ± 5.7	9.0	37.1	15.0 ± 5.6	5.1	28.1	11.3 ± 6.2	2.8	31.4
Copper (Cu)	17 ± 13.8	3.2	59.9	10.4 ± 5.8	3.6	26.2	13.6 ± 13.3	5.2	89.3	17.4 ± 12.9	3.6	70.5
Erbium (Er)	16.1 ± 12.7	4.3	65.8	12.1 ± 12	3.9	55.8	10.9 ± 5.7	<DL	28.2	14.6 ± 8.8	2.2	43.5
Strontium (Sr)	12.2 ± 7.3	3.4	52.0	8.0 ± 5.1	2.8	25.9	7.6 ± 2.6	4.2	14	12.9 ± 9.9	1.4	49.3
Yttrium (Y)	11.3 ± 13	<DL	58.3	5.0 ± 7.3	<DL	39.6	10.2 ± 10.2	<DL	37.3	12.2 ± 14.4	<DL	75
Cerium (Ce)	6.2 ± 5.8	<DL	27.8	9.4 ± 7.9	<DL	40.4	8.5 ± 3.9	<DL	14.1	3.4 ± 3.0	<DL	12.7
Chromium (Cr)	5.2 ± 2.6	1.1	14.1	3.9 ± 3.7	1.1	19.1	3.6 ± 1.8	<DL	9.3	6.4 ± 3.2	2.1	19.5
Water-soluble ions IS (µg/m³)												
Sulfate (SO ₄ ^{2−})	17.8 ± 17	2.9	85.9	8.5 ± 3.2	1.9	22.9	12.1 ± 4.9	4.6	29.3	8.6 ± 4.7	2.1	20.2
Ammonium (NH ₄ ⁺)	2.5 ± 1.9	0.2	8.3	2.4 ± 0.9	0.6	4.9	3.2 ± 1.3	1.2	6.5	3.2 ± 1.7	0.44	7.3
Nitrate (NO ₃ [−])	1.5 ± 0.9	0.1	4.1	1.1 ± 0.8	0.2	3.9	0.9 ± 0.6	0.1	2.3	1.2 ± 0.6	0.4	2.6
Oxalate (C ₂ O ₄ ^{2−})	0.3 ± 0.1	<DL	0.5	0.1 ± 0.1	0.04	0.2	0.1 ± 0.1	0.04	0.3	0.4 ± 0.5	0.02	1.9

Cycle 1 (Spring): 8 April–28 May 2013 (KAH, KFH and Al-Rawda—only the first 10 days were sampled at this site), **Cycle 2 (Summer):** 11 July–24 August 2013 (KAH and KFH), **Cycle 3 (Fall):** 2 October–16 November 2013 (KAH and Al-Rehab/or KAU), **Cycle 4 (Winter):** 7 January 2014–18 February 2014 (KAH and Al-Rehab/or KAU), **DL:** detection limit; **S.D:** standard deviation; **BC:** black carbon; **TEs:** trace elements/metals; **IS:** water-soluble ionic species.

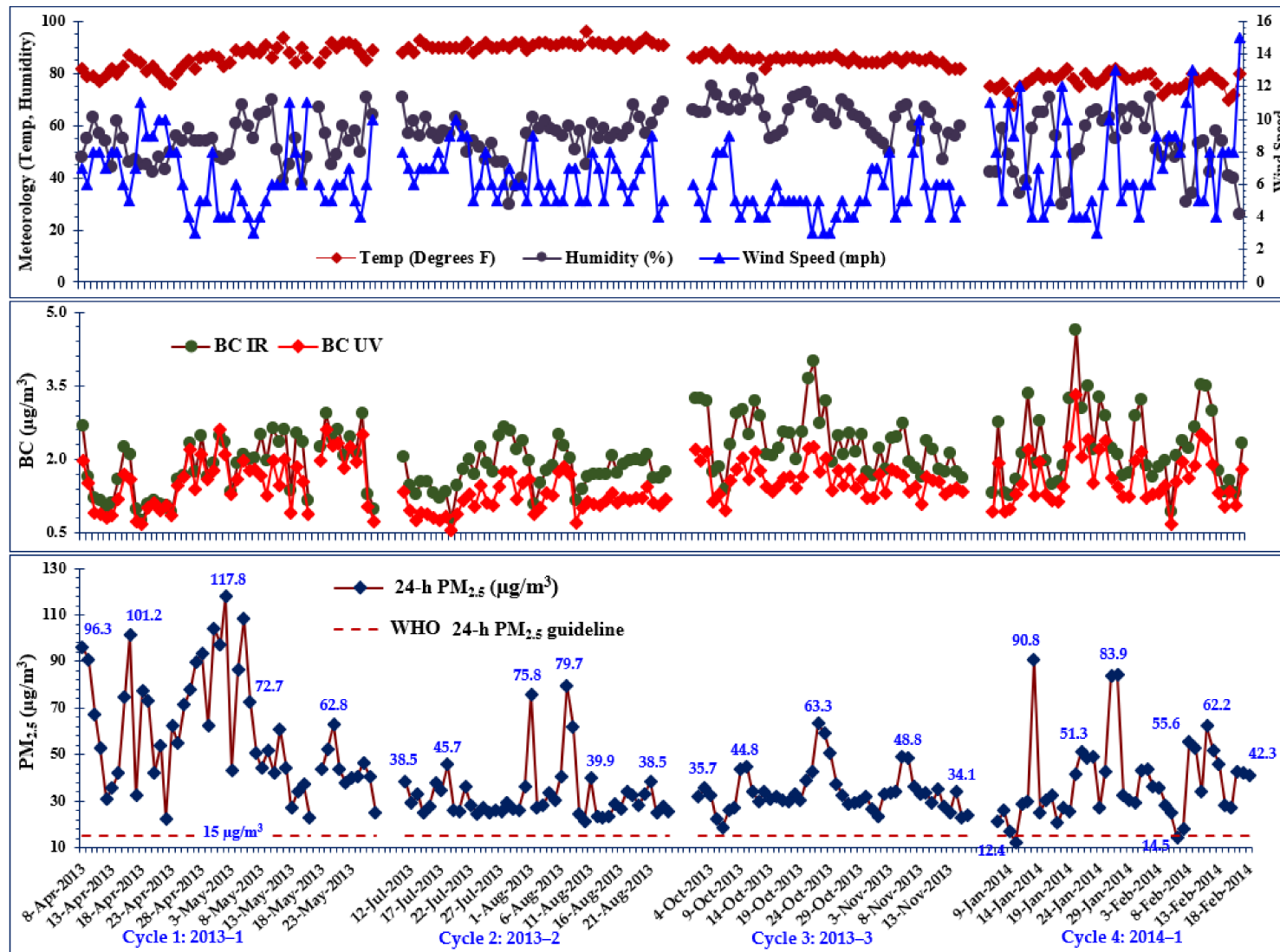


Figure 2. Time-series plots for the 24-h $\text{PM}_{2.5}$, BC, and meteorology during the study period in Jeddah—averaged sampling sites.

3.2. Air Quality Index (AQI) in Jeddah and Comparison with Other Studies

The AQI was calculated [51] based on the observed daily PM_{2.5} levels (Figure 3). The calculated AQI for any given pollutant is always proportional to its levels in the air. Thus, the high AQI values, as seen in this study, simply imply elevated levels of ambient PM_{2.5} in Jeddah. This also translates to a great deal of severe health risk for the exposed population. With exception of cycle 1 that recorded unhealthy to very unhealthy AQI, the general air quality for the rest of the study period was mostly at a moderate level (Figure 3). Notably, we did not observe a single day with good air quality throughout the study period. This further stressed the severity of particulate air pollution in Jeddah and the rest of the Middle East region. Moreover, the AQI in this study was calculated using only the overall PM_{2.5} levels. Thus, we may have potentially underestimated the severity of the observed air pollution levels. Results could possibly show more severe health effects, if additional AQI values based on the gaseous pollutants, such as ozone (O₃) and sulfur dioxide (SO₂), were available. It is also noteworthy that, though the AQI provides a simplified interpretation of the health hazard level associated with an exposure to a given air pollutant, it is not an air quality guideline. Nevertheless, the AQI results can inform the process of policy formulation and implementation.

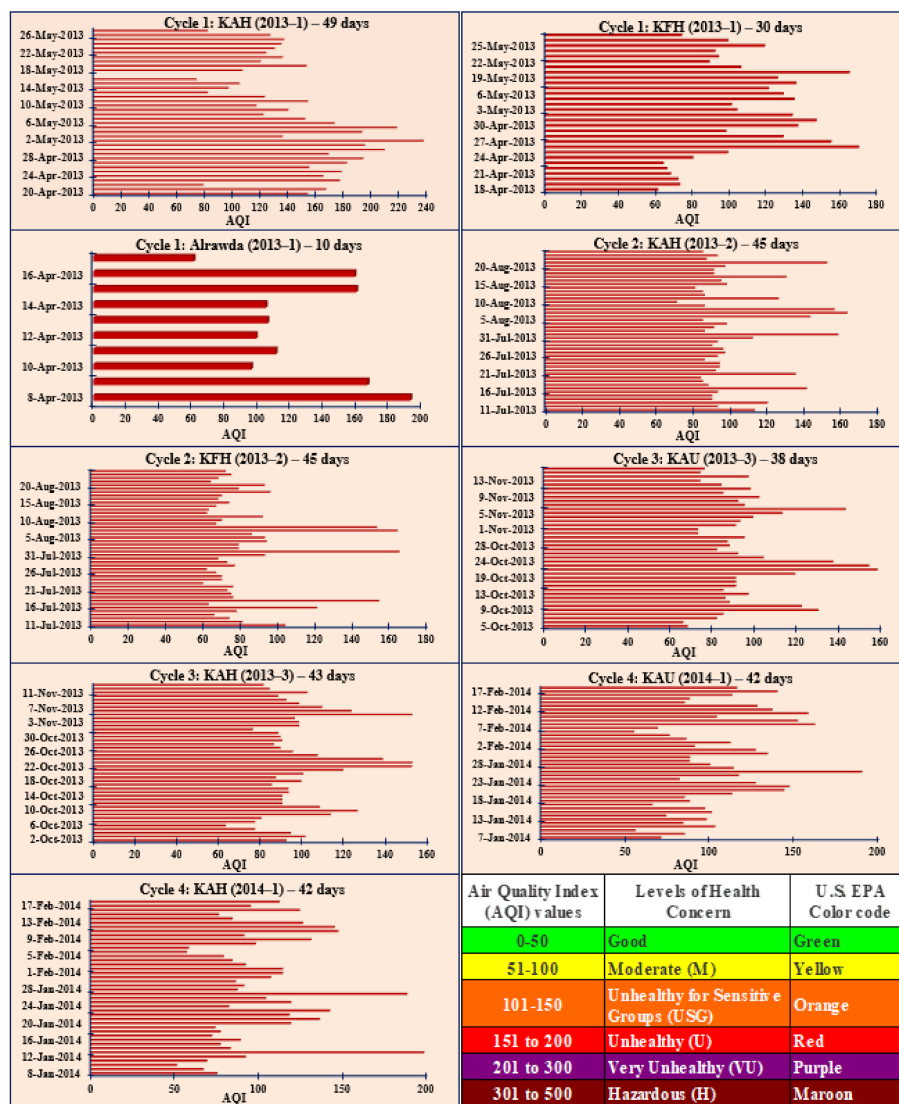


Figure 3. Bar graphs showing the Air Quality Index for PM_{2.5} measured in Jeddah. AQI computations are based on the provisions of the United States Environmental Protection Agency (U.S. EPA).

Furthermore, we compared the recorded daily PM_{2.5} levels with both the WHO and Saudi Arabia's PME guidelines, and the levels recorded in other cities worldwide. The observed mean 24-h PM_{2.5} did not only exceed the 24-h WHO (15 µg/m³) and PME (35 µg/m³) guidelines but were also markedly higher than levels reported for most urban centers of developed countries globally (Figure S2, based on [1,11,12,16,52–65]). Only the major cities in developing countries such as India, China, Pakistan, Bangladesh, and Mongolia, that have historically high levels of air pollution, had PM_{2.5} levels that were either comparable or higher than the levels recorded in this study (Figure S2). This further stressed the extent of particulate air pollution in Jeddah and the rest of the Middle Eastern region.

3.3. PM_{2.5} Mass-Reconstruction

The PM-mass reconstruction tool was utilized to explain the variations between the observed and the expected PM_{2.5} levels. Daily PM_{2.5} was decomposed into five (5) broad pollutants categories as: crustal materials (CMs), secondary ions (SI), sea-sprays (SS), black carbon (BC), and anthropogenic TEs, which we used to explain the variations in daily PM_{2.5}, as presented in Figure 4. Overall, the largest portion (38.7–48.1%) was attributed to SI (SO₄²⁻, NO₃⁻, and NH₄⁺). The precursors of *p*-SO₄²⁻ (SO₂) and *p*-NO₃⁻ (NO_x) are typically linked to fossil-fuel combustion and vehicular emissions. The second largest portion (28.7–42%) was attributed to CMs, especially during cycle 4 (January–February) where CMs comprised the largest proportion (42%) of the overall PM_{2.5}. Jeddah experiences strong winds accompanied by sandstorms during winter and spring seasons [48]. These drastically increase the ambient enrichment of CMs. BC and the anthropogenic TEs also constituted a significant portion of the measured PM_{2.5}, further highlighting the influence of anthropogenic PM emissions in Jeddah. In general, BC, TEs, and SI combined explained 73.6–89.5% of the observed PM_{2.5} (Figure 4).

The estimates of particulate organic matter (POM) were not available for this study. In addition, converting the total S from ED-XRF to SO₄²⁻ (expected) and comparing it with the soluble SO₄²⁻ from IC analysis (observed), showed significant differences per cycle (Table S3). While cycle 1 over-estimated SO₄²⁻, cycles 2–4 showed significant under-estimates of observed SO₄²⁻. This may partially be due to some S-containing compounds not being completely water-soluble [36]. The observed SO₄²⁻ represents only the water-soluble portion. The PM mass closure on SI used the observed SO₄²⁻. The remaining water-insoluble portion and POM account for the unexplained portion of PM_{2.5} during cycles 2–4. Despite the significant over-estimates in SO₄²⁻, cycle 1 still had the largest portion of unexplained PM_{2.5} (26.4%). This may partially be attributed to the missing POM and some measurement errors. Besides being a useful tool for delineation of sources, PM mass-reconstruction can be utilized for assessing the data integrity where significant over- and under-estimates may be revealed by comparing the observed and re-constructed levels of target pollutants, as shown in Figure 4.

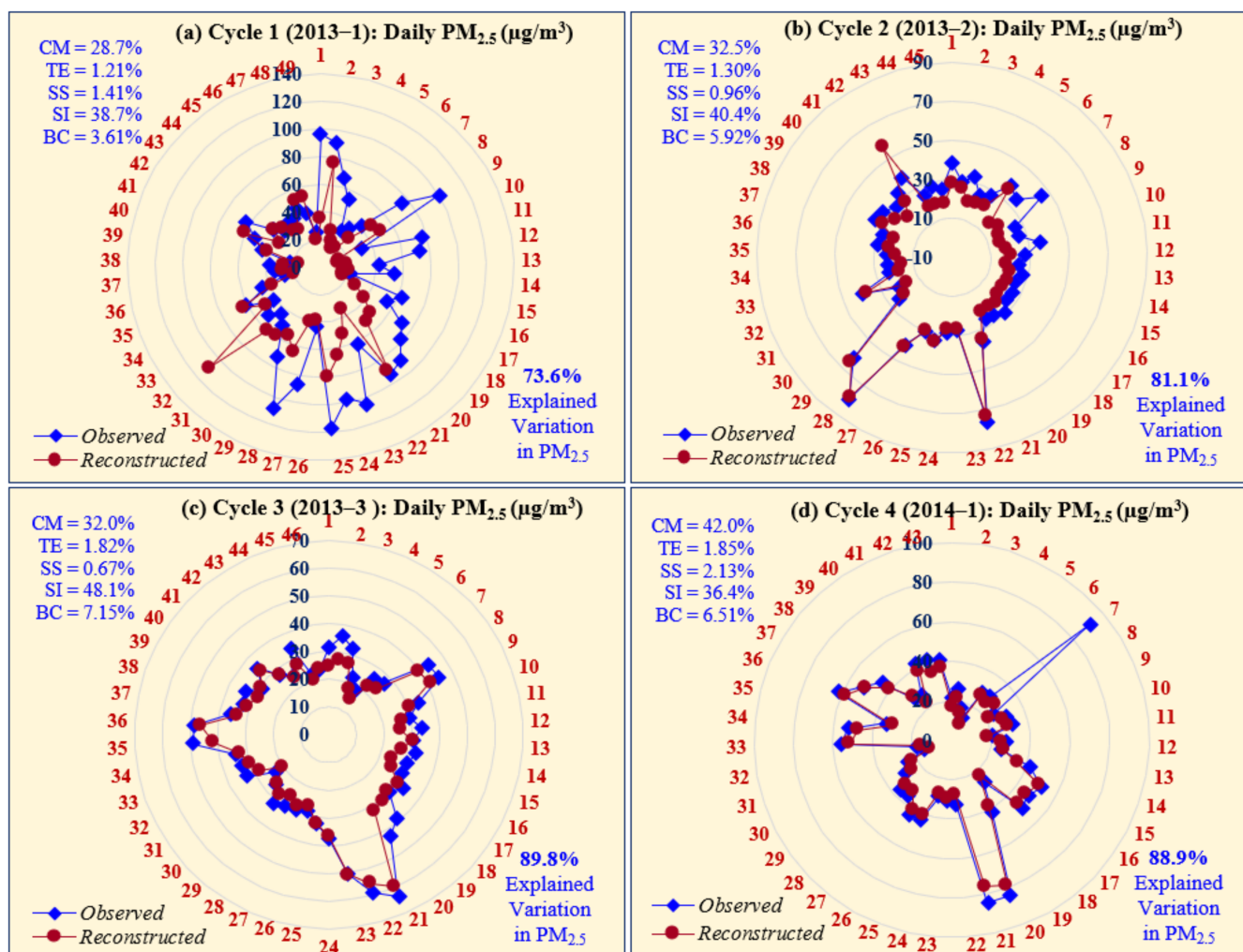


Figure 4. Variations in the observed and reconstructed PM_{2.5} per cycle averaged sampling sites: cycle 1—(a), cycle 2—(b), cycle 3—(c), cycle 4—(d) The relative proportions of daily PM_{2.5} explained by crustal material (CM), trace elements (TE), sea sprays (SS), secondary ions (SI), and black carbon (BC) per cycle are also provided.

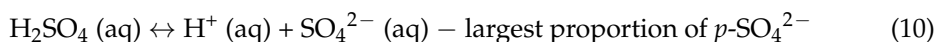
3.4. Correlation between Air Pollutants and Meteorology

Correlations (r) between various pollutants are summarized in Table S4. Pearson's correlation was favored because we wanted to assess the linear relationships between individual pollutant species and meteorology. This is critical to understanding the links between the pollutants measured in PM_{2.5} aerosol, and ultimately, the accurate delineation of their emission sources. Mean daily PM_{2.5} had a weak negative correlation with wind speed (WS) ($r = -0.24$), and temperature ($r = -0.13$), p -value < 0.0001. WS increases the ambient dispersion of PM_{2.5}, while elevated ambient temperatures cause unstable atmospheres and strong convective winds, leading to quick dispersion of PM_{2.5}; thus, the observed negative correlations.

Daily PM_{2.5} was moderately correlated (p -value < 0.0001) with crustal TEs; Mg ($r = 0.67$), Si ($r = 0.66$), Al ($r = 0.63$), K ($r = 0.57$), Ti ($r = 0.43$), Fe ($r = 0.39$), and Ca ($r = 0.33$), indicating a major contribution from the earth crust, as highlighted by the proportion of PM_{2.5} attributed to CM (Figure 4). In addition, PM_{2.5} was moderately correlated with anthropogenic TEs; Ni ($r = 0.53$), Cu ($r = 0.48$), Lu ($r = 0.42$), Zn ($r = 0.32$), and Pb ($r = 0.20$), p -value < 0.0001. Though these TEs accounted for a small portion (1.2–1.9%) of PM_{2.5} (Figure 4), they are good makers for specific anthropogenic sources.

Daily PM_{2.5} had a moderate correlation with $p\text{-SO}_4^{2-}$ ($r = 0.50$, $p\text{-value} < 0.0001$) and not correlated with $p\text{-NO}_3^-$, indicating a major industrial contribution. Jeddah is heavily industrialized, and thus the high emissions of SO₂ are a precursor for the observed high levels of $p\text{-SO}_4^{2-}$ in this study. $p\text{-SO}_4^{2-}$ constituted a major portion of the secondary aerosols (SI).

The daily PM_{2.5} was moderately correlated with $p\text{-NH}_4^+$ ($r = 0.30$), but $p\text{-NH}_4^+$ was highly correlated with $p\text{-SO}_4^{2-}$ ($r = 0.73$), $p\text{-value} < 0.0001$. This high correlation between $p\text{-NH}_4^+$ and $p\text{-SO}_4^{2-}$ is more linked to the fact that both species are mostly formed as fine aerosols, through similar gas-phase reactions, as opposed to having a common source. Moreover, $p\text{-NH}_4^+$ was evidently less than $p\text{-SO}_4^{2-}$ (Table 1) with a molar ratio ($\text{NH}_4^+:\text{SO}_4^{2-}$) of 0.24 (< 2), implying an incomplete neutralization of ambient H₂SO₄. Thus, the available NH₄⁺ salts consisted of a mixture of (NH₄)₂SO₄ and NH₄HSO₄ (Equations (8) and (9)). In addition to the high emission sources, the observed high $p\text{-SO}_4^{2-}$ levels may also be attributed to elevated ambient temperatures, favorable for the photochemical activity and atmospheric oxidation processes; hence, the increased oxidation of SO₂ to $p\text{-SO}_4^{2-}$. Besides, there was barely enough NH₄⁺ to neutralize one quarter of the observed $p\text{-SO}_4^{2-}$. Thus, most of the $p\text{-SO}_4^{2-}$ was likely from ionization of atmospheric H₂SO₄, as shown in Equation (10).



In addition, $p\text{-SO}_4^{2-}$ was moderately correlated with Ni ($r = 0.56$), Cu ($r = 0.38$), Zn ($r = 0.35$), Lu ($r = 0.30$), V ($r = 0.26$), and Pb ($r = 0.24$), $p\text{-value} < 0.0001$, suggesting both a common source and a portion of the observed $p\text{-SO}_4^{2-}$ existing in the form of sulfates of these anthropogenic TEs.

$p\text{-NO}_3^-$ had a moderate negative correlation with $p\text{-NH}_4^+$ ($r = -0.50$), SO_4^{2-} ($r = -0.27$), and a positive correlation with Cl^- ($r = 0.39$). $p\text{-NH}_4^+$ and Cl^- were also negatively correlated ($r = -0.32$), $p\text{-value} < 0.0001$. These negative correlations are indicative of different temporal variabilities. Additionally, this shows that there was no $p\text{-NH}_4^+$ attributable to neutralization of atmospheric HNO₃ and HCl. Thus, the $p\text{-NH}_4^+$ salts did not comprise any NH₄NO₃ and NH₄Cl. Positive correlations between $p\text{-NH}_4^+$, $p\text{-SO}_4^{2-}$, $p\text{-NO}_3^-$, and Cl^- would imply uniform mixing and/or similar gas-phase formation processes.

The $p\text{-NO}_3^-$ is formed either as a coarse or fine aerosol depending on the geographical location and meteorology [66,67]. In marine coastal areas such as Jeddah, there is a high ambient enrichment of Na, K and Mg from the soil and sea-sprays. Indeed, $p\text{-NO}_3^-$ had a moderate correlation with Na ($r = 0.57$), K ($r = 0.32$), and Mg ($r = 0.24$), $p\text{-value} < 0.0001$. Thus, a portion of $p\text{-NO}_3^-$ was in the form of NaNO₃, KNO₃ and Mg(NO₃)₂. These nitrates typically form as coarse aerosols [68]. The fine aerosol mode $p\text{-NO}_3^-$ (NH₄NO₃) only forms in regions with high levels of ambient NH₃ and HNO₃ and low $p\text{-SO}_4^{2-}$ [69]. Once formed, NH₄NO₃ is thermally unstable and exists in a dynamic equilibrium with its precursors (NH₃ and HNO₃). It can only be in aerosol phase at low temperatures [69,70]. Given the high ambient temperatures in this study, NH₄NO₃ would quickly be lost through evaporation and photolytic decomposition upon formation [70]. $p\text{-NO}_3^-$ loss has been reported in several studies [71,72]. We did not explore the dissociation of atmospheric HNO₃, but it is likely that some of the observed $p\text{-NO}_3^-$ was generated from this process.

Black carbon (BC) was moderately correlated with PM_{2.5} ($r = 0.31$), $p\text{-SO}_4^{2-}$ ($r = 0.33$), Ni ($r = 0.47$), Cu ($r = 0.34$), V ($r = 0.27$), and Pb ($r = 0.27$), $p\text{-value} < 0.0001$, suggesting a common emission source with these pollutants and further stressing a major influence from vehicular and industrial emissions.

3.5. Elemental Enrichment Factor (EF)

The distribution of natural and anthropogenic TEs per cycle is presented in Figure 5 and Supplemental Materials (Table S5). Anthropogenic sources as indicated by $EF > 10$, contributed significantly to Ni, V, Cu, Y, Zn, Cl, S, Pb, Br, and Lu; while the earth-crust derived TEs ($EF \leq 10$) included Si, Ti, Fe, Mg, K, Mn, Sr, Ca, Cr, Na, Ce, and Al. Whereas a TE may be classified as earth-crust derived based on the EF value, it is important to note that there could be some proportions coming from the anthropogenic sources. Notably, EF, when combined with other analyses such as PMF, principal component analysis, and chemical mass balance, can be key to defining the overall extent of anthropogenic influence in air pollution research.

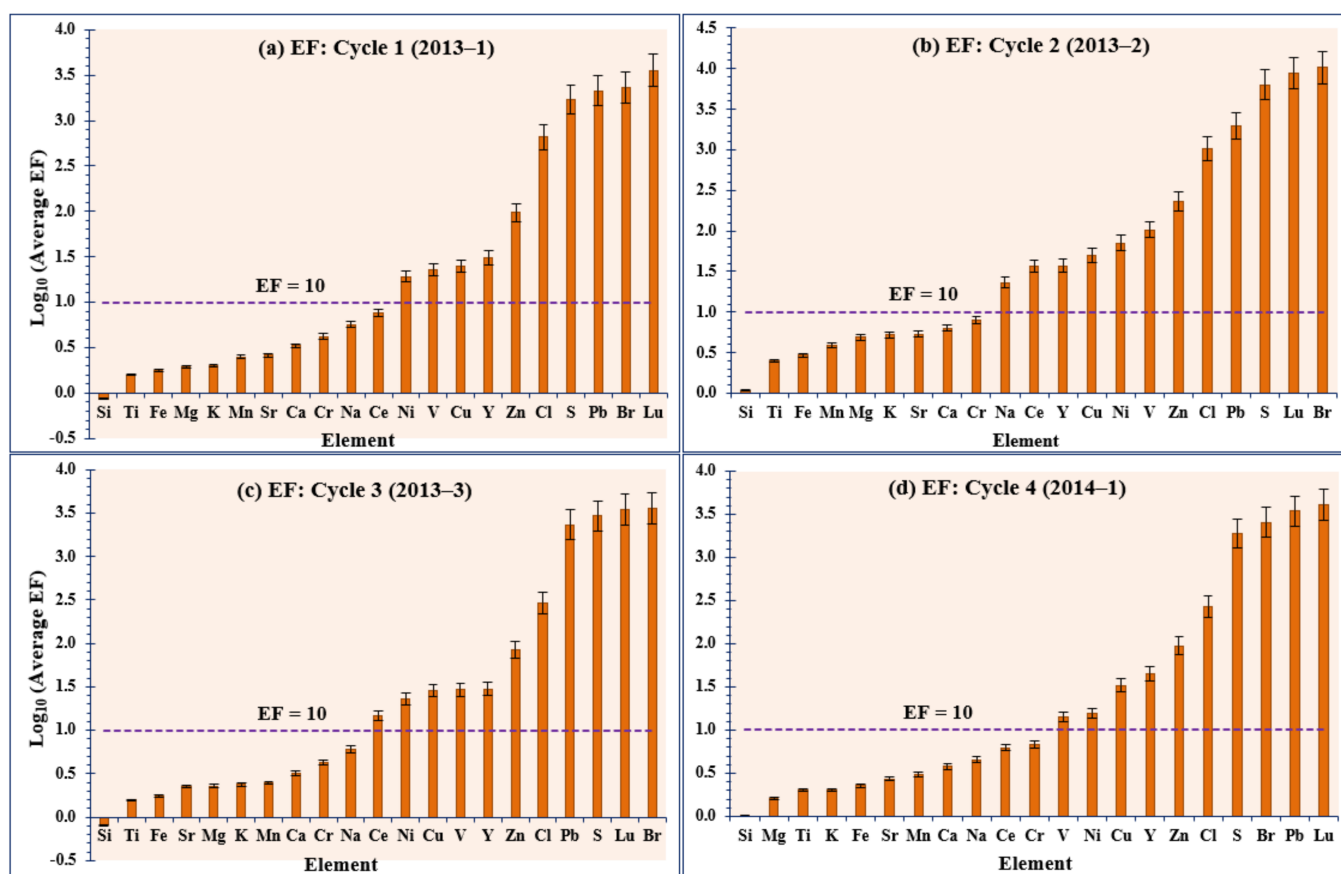


Figure 5. The log transformed enrichment factors (EFs) of trace elements measured from $PM_{2.5}$ per cycle—averaged sampling sites: cycle 1—(a), cycle 2—(b), cycle 3—(c), cycle 4—(d). Elements with EF values exceeding 10 (as indicated by the dotted line), have significant proportions coming from anthropogenic emission sources.

Apart from sulfur (S), anthropogenic TEs contributed a small portion (~1.6%) of the overall $PM_{2.5}$. Though Cl was classified as anthropogenic by EF, Cl is typically associated with marine input as sea-sprays. With Jeddah's location, the contribution of sea-sprays during the study was likely substantial. Vanadium (V) and S are typically associated with oil combustion processes as seen in petrol-chemical industries. V occurs naturally in fossil-fuels, natural oil deposits, and in about 65 different minerals [73], while S is typically emitted as SO_2 from fossil-fuel/oil combustion processes. Copper (Cu), Zn, Ni, Br, and Pb can originate from vehicular emissions [73,74] and several industrial processes (especially Ni and Br). Notably, Cu and Zn have antioxidant properties that attract their use in engine oil. Notably, though Saudi Arabia phased out the use of leaded gasoline in January 2001, as of 2011, the allowable Pb content in gasoline remained at 13 mg/L, which meant that in high traffic density cities the EF of Pb would still be elevated. It was estimated that

total Pb in consumed fuel in Jeddah was about 83.6 tons per year [3,74]. Over the years, with continued implementation of the ban on Pb-gasoline, the current Pb emissions from automobiles are considerably lower. However, the environmental Pb contamination is still an issue and may be attributable to several sources. In addition, the ban on Pb-gasoline implied the phasing out of the use of Br as an essential component of engine anti-knock fluid. However, Br compounds are still being used in batteries of electric cars designed to produce zero BC and NO_x emissions, and several other applications (such as, water treatment, pesticides, and drugs).

Rare earth TEs (Lu, Ce, and Y) were also quantified above their respective limits of quantification (LOQs). Being rare, these elements in PM_{2.5} are typically indicative of anthropogenic applications. For example, the stable isotopes of Lu (¹⁷⁵Lu and ¹⁷⁶Lu) are used as catalysts in petroleum industry for cracking hydrocarbons in oil refineries [1,75], while Ce is used as a fuel additive to cut automobile emissions. The oxides of Ce are also used to catalyze petroleum cracking in petroleum refineries (CeO) [76,77], and as a catalytic converter in automobiles (Ce₂O₃), for oxidation of CO and NO_x emissions [78].

3.6. Positive Matrix Factorization (PMF)

PMF (version 5.0.14) was applied to resolve the emission sources of PM_{2.5} in Jeddah. To improve the study statistical power, we performed the PMF analysis utilizing data from combined cycles. The results are presented in Table 2 and Figures 6 and S3. Due to substantial seasonal variations in pollutant concentrations, we performed additional analyses per cycle, to evaluate seasonal variations in emission sources. Results are presented in Supplemental Materials (Tables S6 and S7 and Figures S4–S7). Sulfur (S) and SO₄²⁻ are basically related since SO₄²⁻ is formed as a secondary aerosol from oxidation of SO₂. However, S from ED–XRF represents the total S, while SO₄²⁻ represents only the water-soluble portion of S. Since there were significant over- and under-estimates in SO₄²⁻ per cycle (Table S3), total S from ED–XRF became more favorable for the PMF analysis. Moreover, though S and SO₄²⁻ were highly correlated (R² = 0.79–0.98), these correlations varied significantly by cycle (Figure S8), making S a better option for the PMF analysis. Oxalate (C₂O₄²⁻) was excluded from PMF analysis due to its low levels in all the samples.

Table 2. Signal-to-noise ratios (S/N), categories, and distribution of residuals for the pollutant species used for positive matrix factorization (PMF) analysis.

Pollutant Species	Category	R ²	Normal Residuals	S/N	Modeled Samples (%)
PM _{2.5}	Weak	0.39	Yes	10	100
Black carbon (BC)	Strong	0.62	Yes	10	100
Sodium (Na)	Strong	0.83	Yes	10	100
Magnesium (Mg)	Strong	0.95	Yes	10	100
Aluminum (Al)	Strong	1.00	Yes	10	100
Silicon (Si)	Strong	1.00	No	10	100
Sulfur (S)	Strong	0.98	No	10	100
Chlorine (Cl)	Strong	1.00	No	6.4	100
Potassium (K)	Strong	0.97	Yes	10	100
Calcium (Ca)	Strong	1.00	Yes	10	100
Titanium (Ti)	Strong	0.99	Yes	10	100
Vanadium (V)	Strong	0.74	No	9.5	100
Chromium (Cr)	Strong	0.71	Yes	8.8	100
Manganese (Mn)	Strong	0.87	Yes	10	100
Iron (Fe)	Strong	0.99	Yes	10	100
Nickel (Ni)	Strong	0.76	Yes	10	100
Copper (Cu)	Strong	0.32	Yes	10	100
Zinc (Zn)	Strong	0.24	No	10	100
Bromine (Br)	Strong	0.03	Yes	9.3	100
Strontium (Sr)	Strong	0.98	Yes	10	100
Yttrium (Y)	Strong	0.08	Yes	7.8	100
Cerium (Ce)	Weak	0.19	Yes	3.0	100
Erbium (Er)	Strong	0.51	No	7.3	100
Lutetium (Lu)	Strong	0.49	No	9.9	100
Lead (Pb)	Strong	0.08	Yes	9.3	100
Ammonium (NH ₄ ⁺)	Strong	0.89	No	9.8	100
Nitrate (NO ₃ ⁻)	Strong	1.00	Yes	10	100

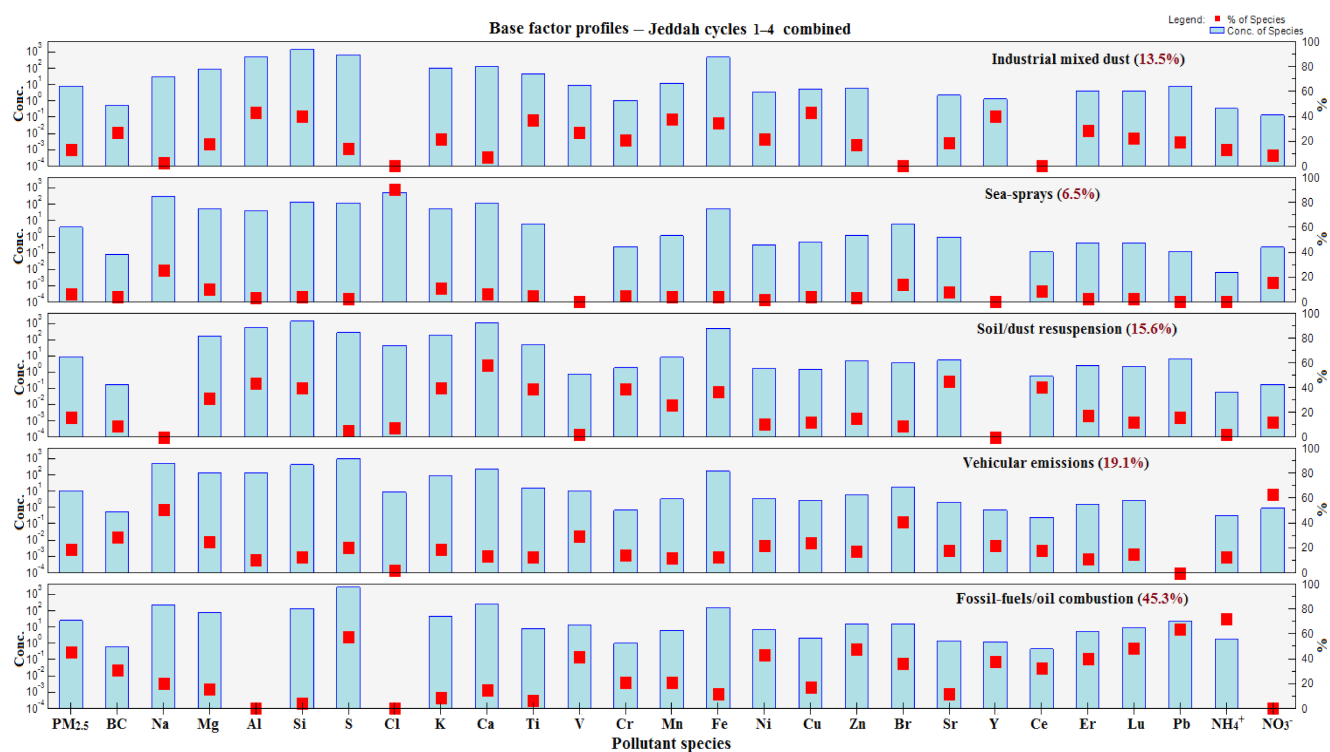


Figure 6. Base factor profiles and contributions to the overall PM_{2.5}—all cycles combined.

A rotational tool (bootstrap analysis) was used to estimate the factor-related uncertainties and assess the rotational uncertainty of our PMF models. We compared the factors between each bootstrap run with the initial PMF output. The PMF solutions that did not attain optimal factor separation (as shown by the residual analyses) were not considered for further analyses. We then used the retained solutions to further test the robustness of our PMF models output(s). Finally, we resolved the PMF base models at 20 runs with five (5) factors. As a quality control and robustness test, we ran/applied the selected base models 5–10 times each, to test the consistency of the results (PMF outputs). Typically, PMF outputs are always consistent and attain a 100% convergence on all the runs when the PMF models are resolved with the correct number of factors.

Overall, the Q-values (Q-robust and Q-true) for all the models were consistent and within a close range, following multiple runs. Given that the Q-robust values are based on the model with controlled outliers, while the Q-true values include outliers, the observed slight differences in the Q-values implied a perfect fit for the data within each model. Additionally, all the models attained a 100% convergence rate on all the runs, and thus alluding more to the accuracy of the number of factors used. The presented PMF results are based on the run with the lowest Q-robust value. However, given the minor differences in the Q-values, results were similar for all the runs.

From the diagnostics data (residual analyses), most of the pollutant species had normally distributed residuals and relatively high signal-to-noise ratios (S/N), except Ce (Table 2). Thus, Ce was classified as “weak”, to limit its influence on the results. Additionally, since we were delineating the PM_{2.5} emission sources, PM_{2.5} as a parameter was categorized as “weak” to restrict it from strongly influencing the model results. Pollutant species with S/N > 5 were all classified as “strong” (Tables 2 and S7).

The interpretation of factors to determine the PM_{2.5} emission sources was done by comparing the factor loadings in the profiles of each pollutant specie, as presented in Figures 6 and S3. The chemical components of PM_{2.5} originate from specific sources as discussed in previous sections, and thus can be used as markers for source identification.

Overall, the five delineated PM_{2.5} sources in Jeddah were: (1) *fossil-fuels/oil combustion* (45.3%)—S, V, Pb, Ni, Lu, Zn, Br, Y, and BC; (2) *vehicular emissions* (19.1%)—NO₃[−], Br, Cu,

Zn, Ni, V, S, Mg, Na, and BC; (3) *soil/dust resuspension* (15.6%)—Mg, Al, Si, K, Ca, Ti, Cr, Mn, Fe, Zn, Sr, Er and Pb; (4) *industrial mixed dust* (13.5%)—Mg, Al, Si, S, K, Ti, V, Cr, Mn, Fe, Ni, Cu, Zn, Sr, Y, Er, Lu, Pb and BC. Jeddah has several industries and heavy vehicular traffic. The industrial dust contained a mixture of pollutants emitted from several anthropogenic activities; and (5) *sea-spray* (6.5%)—Cl, Na, Mg, K, and Ca. Jeddah's location at the coast of the Red Sea, makes the contribution from sea-sprays to the overall air pollution significant.

3.7. Backward-In-Time Trajectories

Plots of wind trajectories 72 h prior to sampling for the two days with the highest and lowest PM_{2.5} levels per cycle are presented under Supplemental Materials (Figures S9–S12). The days with wind flowing over the Red Sea into Jeddah had the lowest PM_{2.5}. Ideally, the air above the sea has lower PM levels, which introduces a dilution effect. Conversely, wind flowing over inland areas into Jeddah had higher PM_{2.5}. Jeddah and the neighboring cities of Makkah, Medina, and Rabigh are heavily industrialized. This presented an opportunity to pick up pollutants from these neighboring cities into Jeddah. This also further highlights the significance of local and regional emissions to the PM_{2.5} levels in Jeddah.

Notably, during cycle 4 (Figure S12), one of the days with high PM_{2.5} (27 January 2014) had wind trajectories passing over the Red Sea. On this day, the southeasterly gusty winds originating from the Gulf of Eden were associated with a dust-storm event from 12:00 pm to 19:00 pm which contributed to the high PM_{2.5} levels observed on that day.

Overall, across the study period, the wind trajectories indicated that local and regional emissions, as well as the long-distance transport, may have contributed significantly to the observed PM_{2.5}.

4. Conclusions

This is a comprehensive assessment of PM_{2.5} air pollution, providing a thorough delineation of the major emission sources in Jeddah. The observed PM_{2.5} levels exceeded the WHO (15 µg/m³) and Saudi Arabia's PME (35 µg/m³) guidelines, stressing a major pollution issue. Results highlight a significant anthropogenic influence on air pollution levels in Jeddah and thus, will be key to refining the local policies on air pollution. From delta-C estimates, results indicated little to no PM_{2.5} emissions from biomass combustion. Conversely, the estimates of *p*-SO₄²⁻, *p*-NO₃⁻, and *p*-NH₄⁺ were significantly high, indicating major PM_{2.5} emissions from industrial and automobile sources. Furthermore, EF defined several anthropogenic TEs (Ni, V, Cu, Zn, Pb, S, Lu, and Br) that were intricately linked to industrial and automobile emissions. Further analyses from PMF resolved five (5) major sources including: *fossil-fuels/oil combustion* (45.3%), *vehicular emissions* (19.1%), *soil/dust resuspension* (15.6%), *industrial mixed dust* (13.5%) and *sea-spray* (6.5%).

Anthropogenic sources contributed ~78% of the measured PM_{2.5} with the largest proportions coming from industrial and vehicular emissions. Thus, future policies on particulate air pollution may need to target these two sources. Furthermore, given the existing body of evidence of adverse health outcomes at much lower exposure levels than reported in this study, the current PME guideline on PM_{2.5} needs to be revised to lower the acceptable levels as well as enforce strict compliance. Introduction of go-green policies in mass transit systems may be a great idea. Go-green policies may involve the electrification and hybridization of the existing transport modes, to reduce the overdependency on petroleum, and thus lower the BC and NO_x emissions.

Notably, the wind trajectories highlighted a possible major pollution contribution from regional and long-distance transport. Thus, a regional approach to air pollution control will be more beneficial and effective, given the long-distance transport. In addition, as per the suggestion from the reviewers, future studies utilizing wind trajectories may need to incorporate additional receptor analyses based on hybrid receptor models (such as the potential source contribution function (PSCF) model, CWT, etc.) to analyze the spatial distribution and ultimately quantify the contribution from regional/long-distance transport. These models are applicable on both the PM_{2.5} and PMF reconstructed sources that are

potentially influenced by wind transport. This is a key feature for further assessment of the potential contribution of long-distance transport to the observed PM_{2.5} levels.

Overall, our results supplement the previously published data, and further highlight the need for more research to fully appreciate the major air pollution related issues in Saudi Arabia. This is key to both the formulation and enactment of sustainable policies on air pollution for the entire Middle East region.

Supplementary Materials: The following supporting information can be downloaded at: <https://www.mdpi.com/article/10.3390/atmos13050711/s1>, Figure S1: An assembled PM_{2.5} sampler showing the major components—Photo by author(s); Figure S2: Comparison of mean PM_{2.5} levels measured in Jeddah with other cities worldwide; Figure S3: Factor fingerprints and contributions to the overall PM_{2.5} in Jeddah—combined cycles; Figure S4: Base factor profiles and contributions to the overall PM_{2.5}—Jeddah cycle 1; Figure S5: Base factor profiles and contributions to the overall PM_{2.5}—Jeddah cycle 2; Figure S6: Base factor profiles and contributions to the overall PM_{2.5}—Jeddah cycle 3; Figure S7: Base factor profiles and contributions to the overall PM_{2.5}—Jeddah cycle 4; Figure S8: Plots of water-soluble SO₄^{2−} from IC analysis versus total S from ED-XRF analysis; Figure S9: Plots of backward-in-time wind trajectories showing wind direction and its influence on daily PM_{2.5} measured in Jeddah (cycle 1); Figure S10: Plots of backward-in-time wind trajectories showing wind direction and its influence on daily PM_{2.5} measured in Jeddah (cycle 2); Figure S11: Plots of backward-in-time wind trajectories showing wind direction and its influence on daily PM_{2.5} measured in Jeddah (cycle 3); Figure S12: Plots of backward-in-time wind trajectories showing wind direction and its influence on daily PM_{2.5} measured in Jeddah (cycle 4); Table S1: Summary of the optimum conditions for analysis of water-soluble cations and anions by ion exchange chromatography; Table S2: Typical detection limits of elements measured on a Thermo Scientific™ ARL™ QUANT'X ED-XRF Spectrometer; Table S3: Summary of the overall variations in expected and observed SO₄^{2−}, NH₄⁺ and NO₃[−] during the four sampling cycles in Jeddah, Saudi Arabia; Table S4: Pearson correlations between different pollutant species measured from PM_{2.5} and with meteorology; Table S5: Mean values for the elemental enrichment factors (EFs) per study cycle; Table S6: Summary of the PMF solution in Jeddah: Sources of PM_{2.5} and their overall relative contributions; Table S7: Signal-to-Noise ratios (S/N) and classifications/categories of air pollutant species used for PMF analysis per cycle in Jeddah.

Author Contributions: Data analysis and organization, interpretation of data, writing original draft, S.R.N.; project administration, funding, review of data, O.S.A.; field measurements, data review, A.S.; experimental execution, M.M.H.; field measurements, J.Z.; software, F.K.; data review and editing, D.O.C.; data review and editing, D.R.B.; conceptualization, supervision, methodology, review, and editing, H.A.K. All authors have read and agreed to the published version of the manuscript.

Funding: This work was supported by a grant from King Abdul-Aziz University, Jeddah, Saudi Arabia.

Institutional Review Board Statement: Not applicable.

Informed Consent Statement: Not applicable.

Data Availability Statement: Not applicable.

Acknowledgments: This research was supported by a grant from King Abdul-Aziz University, Jeddah, Saudi Arabia. The authors are also grateful to Dr. Lung C. Chen, of New York University, School of Medicine, for his support analyzing trace elements by ED-XRF. The authors would also like to acknowledge the contribution of peer reviewer(s) that significantly improved the quality of this publication.

Conflicts of Interest: The authors declare no conflict of interest.

References

1. Nayebare, S.R.; Aburizaiza, O.S.; Khwaja, H.A.; Siddique, A.; Hussain, M.M.; Zeb, J.; Khatib, F.; Carpenter, D.O.; Blake, D.R. Chemical Characterization and Source Apportionment of PM_{2.5} in Rabigh, Saudi Arabia. *Aerosol Air Qual. Res.* **2016**, *16*, 3114–3129. [[CrossRef](#)]
2. Alharbi, B.; Shareef, M.M.; Husain, T. Study of chemical characteristics of particulate matter concentrations in Riyadh, Saudi Arabia. *Atmos. Pollut. Res.* **2015**, *6*, 88–98. [[CrossRef](#)]

3. Khodeir, M.; Shamy, M.; Alghamdi, M.; Zhong, M.; Sun, H.; Costa, M.; Chen, L.-C.; Maciejczyk, P. Source Apportionment and Elemental Composition of PM_{2.5} and PM₁₀ in Jeddah City, Saudi Arabia. *Atmos. Pollut. Res.* **2012**, *3*, 331–340. [[CrossRef](#)] [[PubMed](#)]
4. Munir, S.; Habeebullah, T.M.; Seroji, A.R.; Gabr, S.S.; Mohammed, A.M.F.; Morsy, E.A. Modeling Particulate Matter Concentrations in Makkah, Applying a Statistical Modeling Approach. *Aerosol Air Qual. Res.* **2013**, *13*, 901–910. [[CrossRef](#)]
5. WHO. The World Health Organization (WHO) Air Quality Guidelines–Global Update 2021: Ambient (Outdoor) Air Quality and Health. 2021. Available online: [https://www.who.int/news-room/fact-sheets/detail/ambient-\(outdoor\)-air-quality-and-health](https://www.who.int/news-room/fact-sheets/detail/ambient-(outdoor)-air-quality-and-health) (accessed on 29 March 2022).
6. PME. Presidency of Meteorology and Environment (PME), Ambient Air Quality Standards. Available online: http://www.pme.gov.sa/en/En_EnvStand19.pdf (accessed on 12 April 2016).
7. Nayebar, S.R. *Fine Particulate Air Pollution in Saudi Arabia–Implications for Cardiopulmonary Morbidity*; State University of New York: Albany, NY, USA, 2016.
8. Nasrallah, M.M.; Seroji, A.R. Particulates in the Atmosphere of Makkah and Mina Valley during Ramadhan and Hajj Season of 1424 and 1425 H (2004–2005). *Arab Gulf J. Sci. Res.* **2008**, *26*, 199–206.
9. Khreis, H.; Cirach, M.; Mueller, N.; Hoogh, K.D.; Hoek, G.; Nieuwenhuijsen, M.J.; Rojas-Rueda, D. Outdoor air pollution and the burden of childhood asthma across Europe. *Eur. Respir. J.* **2019**, *54*, 1802194. [[CrossRef](#)]
10. Guerreiro, C.B.B.; Foltescu, V.; De Leeuw, F. Air quality status and trends in Europe. *Atmos. Environ.* **2014**, *98*, 376–384. [[CrossRef](#)]
11. Sillanpää, M.; Frey, A.; Hillamo, R.; Pennanen, A.S.; Salonen, R.O. Organic, elemental and inorganic carbon in particulate matter of six urban environments in Europe. *Atmos. Chem. Phys.* **2005**, *5*, 2869–2879. [[CrossRef](#)]
12. Anderson, H.; Bremner, S.; Atkinson, R.; Harrison, R.; Walters, S. Particulate matter and daily mortality and hospital admissions in the west midlands conurbation of the United Kingdom: Associations with fine and coarse particles, black smoke and sulphate. *Occup. Environ. Med.* **2001**, *58*, 504–510. [[CrossRef](#)]
13. Sheffield, P.E.; Speranza, R.; Chiu, Y.-H.M.; Hsu, H.-H.L.; Curtin, P.C.; Renzetti, S.; Pajak, A.; Coull, B.; Schwartz, J.; Kloog, I.; et al. Association between particulate air pollution exposure during pregnancy and postpartum maternal psychological functioning. *PLoS ONE* **2018**, *13*, e0195267. [[CrossRef](#)]
14. Crouse, D.L.; Peters, P.A.; Van Donkelaar, A.; Goldberg, M.S.; Villeneuve, P.J.; Brion, O.; Khan, S.; Atari, D.O.; Jerrett, M.; Pope, C.A.; et al. Risk of Nonaccidental and Cardiovascular Mortality in Relation to Long-term Exposure to Low Concentrations of Fine Particulate Matter: A Canadian National-Level Cohort Study. *Environ. Health Perspect.* **2012**, *120*, 708–714. [[CrossRef](#)] [[PubMed](#)]
15. Weuve, J.; Puett, R.C.; Schwartz, J.; Yanosky, J.D.; Laden, F.; Grodstein, F. Exposure to Particulate Air Pollution and Cognitive Decline in Older Women. *Arch. Intern. Med.* **2012**, *172*, 219–227. [[CrossRef](#)] [[PubMed](#)]
16. Bell, M.L.; Dominici, F.; Ebisu, K.; Zeger, S.L.; Samet, J.M. Spatial and Temporal Variation in PM_{2.5} Chemical Composition in the United States for Health Effects Studies. *Environ. Health Perspect.* **2007**, *115*, 989–995. [[CrossRef](#)] [[PubMed](#)]
17. Pope, C.A.; Turner, M.C.; Burnett, R.T.; Jerrett, M.; Gapstur, S.M.; Diver, W.R.; Krewski, D.; Brook, R.D. Relationships between fine particulate air pollution, cardiometabolic disorders, and cardiovascular mortality. *Circ. Res.* **2015**, *116*, 108–115. [[CrossRef](#)] [[PubMed](#)]
18. Brook, R.; Rajagopalan, S.; Pope, C.; Brook, J.; Bhatnagar, A.; Diez-Roux, A.; Holguin, F.; Hong, Y.; Luepker, R.; Mittleman, M.; et al. Particulate matter air pollution and cardiovascular disease: An update to the scientific statement from the American Heart Association. *Circulation* **2010**, *121*, 2331–2378. [[CrossRef](#)]
19. Pope, C.A.I.; Dockery, D.W. Health Effects of Fine Particulate Air Pollution: Lines that Connect. *J. Air Waste Manag. Assoc.* **2006**, *56*, 709–742. [[CrossRef](#)]
20. Pope, C.A.; Burnett, R.T.; Thurston, G.D.; Thun, M.J.; Calle, E.E.; Krewski, D.; Godleski, J.J. Cardiovascular Mortality and Long-Term Exposure to Particulate Air Pollution: Epidemiological Evidence of General Pathophysiological Pathways of Disease. *Circulation* **2004**, *109*, 71–77. [[CrossRef](#)]
21. Peden, D.B. The epidemiology and genetics of asthma risk associated with air pollution. *J. Allergy Clin. Immunol.* **2005**, *115*, 213–219. [[CrossRef](#)]
22. Sunyer, J.; Schwartz, J.; Tobias, A.; Macfarlane, D.; Garcia, J.; Antó, J.M. Patients with Chronic Obstructive Pulmonary Disease Are at Increased Risk of Death Associated with Urban Particle Air Pollution: A Case-Crossover Analysis. *Am. J. Epidemiol.* **2000**, *151*, 50–56. [[CrossRef](#)]
23. SADP. *Saudi Arabia Demographic Profile 2014*; PopulationPyramid.Net: Saudi Arabia, 2014.
24. Hasanean, H.; Almazroui, M. Rainfall: Features and Variations over Saudi Arabia, A Review. *Climate* **2015**, *3*, 578. [[CrossRef](#)]
25. Ahmed, T.; Dutkiewicz, V.A.; Shareef, A.; Tuncel, G.; Tuncel, S.; Husain, L. Measurement of black carbon (BC) by an optical method and a thermal-optical method: Intercomparison for four sites. *Atmos. Environ.* **2009**, *43*, 6305–6311. [[CrossRef](#)]
26. Rattigan, O.V.; Civerolo, K.; Doraiswamy, P.; Felton, H.D.; Hopke, P.K. Long term black carbon measurements at two urban locations in New York. *Aerosol Air Qual. Res.* **2013**, *13*, 1181–1196. [[CrossRef](#)]
27. Wang, Y.; Hopke, P.K.; Rattigan, O.V.; Chalupa, D.C.; Utell, M.J. Multiple-year black carbon measurements and source apportionment using Delta-C in Rochester, New York. *J. Air Waste Manag. Assoc.* **2012**, *62*, 880–887. [[CrossRef](#)] [[PubMed](#)]
28. Shaltout, A.A.; Boman, J.; Al-Malawi, D.A.R.; Shehadeh, Z.F. Elemental Composition of PM_{2.5} Particles Sampled in Industrial and Residential Areas of Taif, Saudi Arabia. *Aerosol Air Qual. Res.* **2013**, *13*, 1356–1364. [[CrossRef](#)]

29. Yatkin, S.; Gerboles, M.; Borowiak, A. Evaluation of standardless EDXRF analysis for the determination of elements on PM₁₀ loaded filters. *Atmos. Environ.* **2012**, *54*, 568–582. [CrossRef]
30. Xu, H.M.; Cao, J.J.; Ho, K.F.; Ding, H.; Han, Y.M.; Wang, G.H.; Chow, J.C.; Watson, J.G.; Khol, S.D.; Qiang, J.; et al. Lead concentrations in fine particulate matter after the phasing out of leaded gasoline in Xi'an, China. *Atmos. Environ.* **2012**, *46*, 217–224. [CrossRef]
31. Korzhova, E.N.; Kuznetsova, O.V.; Smagunova, A.N.; Stavitskaya, M.V. Determination of inorganic pollutants in atmospheric aerosols. *J. Anal. Chem.* **2011**, *66*, 222–240. [CrossRef]
32. Margui, E.; Van Grieken, R. *X-ray Fluorescence Spectrometry and Related Techniques*; Momentum Press, LLC.: New York, NY, USA, 2013.
33. Buhrke, V.E.; Jenkins, R.; Smith, D.K. *Practical Guide for the Preparation of Specimens for X-ray Fluorescence and X-ray Diffraction Analysis*; Wiley: Hoboken, NJ, USA, 1998.
34. Thermo-Scientific. Analysis of Air Filters by ARL QUANT'X High Performance Energy Dispersive X-ray Fluorescence Spectrometer (EDXRF). 2007. Available online: <https://www.thermofisher.com/document-connect/document-connect.html?url=https%3A%2F%2Fassets.thermofisher.com%2FTFS-Assets%2FMSD%2FApplication-Notes%2FXRAN41964-air-filter-analysis-EDXRF.pdf> (accessed on 29 March 2022).
35. Chow, J.C.; Lowenthal, D.; Chen, L.W.A.; Wang, X.; Watson, J. Mass reconstruction methods for PM_{2.5}: A review. *Air Qual. Atmos. Health* **2015**, *8*, 243–263. [CrossRef]
36. Watson, J.G.; Chow, J.C.; Lowenthal, D.H.; Chen, L.-W.A.; Wang, X.; Biscay, P. *Reformulation of PM_{2.5} Mass Reconstruction Assumptions for the San Joaquin Valley Final Report*; Desert Research Institute, Nevada System of Higher Education: Reno, NV, USA, 2012.
37. Macias, E.S.; Zwicker, J.O.; Ouimette, J.R.; Hering, S.V.; Friedlander, S.K.; Cahill, T.A.; Kuhlmeier, G.A.; Richards, L.W. Regional haze case studies in the southwestern US—I. Aerosol chemical composition. *Atmos. Environ.* (1967) **1981**, *15*, 1971–1986. [CrossRef]
38. Solomon, P.A.; Fall, T.; Salmon, L.; Cass, G.R.; Gray, H.A.; Davidson, A. Chemical characteristics of PM₁₀ aerosols collected in the Los Angeles area. *JAPCA* **1989**, *39*, 154–163. [CrossRef]
39. Seinfeld, J.H.; Pandis, S.N. *Atmospheric Chemistry and Physics: From Air Pollution to Climate Change*; John Wiley & Sons: Hoboken, NJ, USA, 2012.
40. Fabretti, J.-F.; Sauret, N.; Gal, J.-F.; Maria, P.-C.; Schärer, U. Elemental characterization and source identification of PM_{2.5} using Positive Matrix Factorization: The Malraux road tunnel, Nice, France. *Atmos. Res.* **2009**, *94*, 320–329. [CrossRef]
41. Sofowote, U.M.; McCarry, B.E.; Marvin, C.H. Source Apportionment of PAH in Hamilton Harbour Suspended Sediments: Comparison of Two Factor Analysis Methods. *Environ. Sci. Technol.* **2008**, *42*, 6007–6014. [CrossRef] [PubMed]
42. Hopke, P.K. *A Guide to Positive Matrix Factorization (PMF)*; Center for Air Resources Engineering and Science, Clarkson University: Potsdam, NY, USA, 2000; pp. 1–16.
43. Vivone, G.; D'Amico, G.; Summa, D.; Lolli, S.; Amodeo, A.; Bortoli, D.; Pappalardo, G. Atmospheric Boundary Layer height estimation from aerosol lidar: A new approach based on morphological image processing techniques-(Preprint). *Atmos. Chem. Phys.* **2020**, *21*, 4249–4265. [CrossRef]
44. Ramana, M.V.; Krishnan, P.; Nair, S.M.; Kunhikrishnan, P.K. Thermodynamic structure of the Atmospheric Boundary Layer over the Arabian Sea and the Indian Ocean during pre-INDOEX and INDOEX-FFP campaigns. *Ann. Geophys.* **2004**, *22*, 2679–2691. [CrossRef]
45. Li, W. *Study of Diurnal Cycle Variability of Planetary Boundary Layer Characteristics over the Red Sea and Arabian Peninsula*; King Abdullah University of Science and Technology (KAUST): Thuwal, Saudi Arabia, 2012. [CrossRef]
46. Draxler, R.R.; Rolph, G.D. HYSPLIT (HYbrid Single-Particle Lagrangian Integrated Trajectory) Model Access via NOAA ARL READY Website. NOAA Air Resources Laboratory, College Park, MD. Available online: <http://www.arl.noaa.gov/HYSPLIT.php> (accessed on 13 July 2021).
47. Rolph, G.D. Real-Time Environmental Applications and Display sYstem (READY) Website. NOAA Air Resources Laboratory, College Park, MD. Available online: <http://www.ready.noaa.gov> (accessed on 13 July 2021).
48. Jish Prakash, P.; Stenchikov, G.; Kalenderski, S.; Osipov, S.; Bangalath, H. The impact of dust storms on the Arabian Peninsula and the Red Sea. *Atmos. Chem. Phys.* **2015**, *15*, 199–222. [CrossRef]
49. Singh, N.; Murari, V.; Kumar, M.; Barman, S.C.; Banerjee, T. Fine particulates over South Asia: Review and meta-analysis of PM_{2.5} source apportionment through receptor model. *Environ. Pollut.* **2017**, *223*, 121–136. [CrossRef] [PubMed]
50. Jennifer, G.; Paul, K. *Preliminary Examination of Trace Elements in Tyres, Brake Pads and Road Bitumen in New Zealand*; Ministry of Transport: Wellington, New Zealand, 2003.
51. U.S.EPA. *The National Ambient Air Quality Standards for Particle Pollution. Revised Air Quality Standards for Particle Pollution and Updates to the Air Quality Index (AQI)*; U.S.EPA: Washington, DC, USA, 2012.
52. Zhao, X.; Zhang, X.; Xu, X.; Xu, J.; Meng, W.; Pu, W. Seasonal and diurnal variations of ambient PM_{2.5} concentration in urban and rural environments in Beijing. *Atmos. Environ.* **2009**, *43*, 2893–2900. [CrossRef]
53. Begum, B.A.; Hossain, A.; Nahar, N.; Markwitz, A.; Hopke, P.K. Organic and black carbon in PM_{2.5} at an urban site at Dhaka, Bangladesh. *Aerosol Air Qual. Res.* **2012**, *12*, 1062–1072. [CrossRef]
54. Amarsaikhan, D.; Battsengel, V.; Nergui, B.; Ganzorig, M.; Bolor, G. A Study on Air Pollution in Ulaanbaatar City, Mongolia. *J. Geosci. Env. Prot.* **2014**, *2*, 123. [CrossRef]
55. Kulshrestha, A.; Satsangi, P.G.; Masih, J.; Taneja, A. Metal concentration of PM_{2.5} and PM₁₀ particles and seasonal variations in urban and rural environment of Agra, India. *Sci. Total Environ.* **2009**, *407*, 6196–6204. [CrossRef] [PubMed]

56. Hamad, S.H.; Schauer, J.J.; Heo, J.; Kadhim, A.K.H. Source apportionment of PM_{2.5} carbonaceous aerosol in Baghdad, Iraq. *Atmos. Res.* **2015**, *156*, 80–90. [[CrossRef](#)]
57. Yatkin, S.; Bayram, A. Source apportionment of PM₁₀ and PM_{2.5} using positive matrix factorization and chemical mass balance in Izmir, Turkey. *Sci. Total Environ.* **2008**, *390*, 109–123. [[CrossRef](#)] [[PubMed](#)]
58. Kermani, M.; Arfaeina, H.; Nabizadeh, R.; Alimohammadi, M.; Aalamolhoda, A. Levels of PM_{2.5}—associated heavy metals in the ambient air of Sina hospital district, Tehran, Iran. *J. Air Pollut. Health* **2015**, *1*, 1–6.
59. Brown, K.W.; Bouhamra, W.; Lamoureux, D.P.; Evans, J.S.; Koutrakis, P. Characterization of Particulate Matter for Three Sites in Kuwait. *J. Air Waste Manag. Assoc.* **2008**, *58*, 994–1003. [[CrossRef](#)]
60. Degobbi, C.; Lopes, F.D.; Carvalho-Oliveira, R.; Muñoz, J.E.; Saldiva, P.H. Correlation of fungi and endotoxin with PM_{2.5} and meteorological parameters in atmosphere of Sao Paulo, Brazil. *Atmos. Environ.* **2010**, *45*, 2277–2283. [[CrossRef](#)]
61. Akyuz, M.; Cabuk, H. Meteorological variations of PM_{2.5}/PM₁₀ concentrations and particle-associated polycyclic aromatic hydrocarbons in the atmospheric environment of Zonguldak, Turkey. *J. Hazard Mater.* **2009**, *170*, 13–21. [[CrossRef](#)]
62. Nakhle, M.M.; Farah, W.; Ziade, N.; Abboud, M.; Coussa-Koniski, M.L.; Annesi-Maesano, I. Beirut Air Pollution and Health Effects—BAPHE study protocol and objectives. *Multidiscip. Respir. Med.* **2015**, *10*, 21. [[CrossRef](#)]
63. Hueglin, C.; Gehrig, R.; Baltensperger, U.; Gysel, M.; Monn, C.; Vonmont, H. Chemical characterization of PM_{2.5}, PM₁₀ and coarse particles at urban, near-city and rural sites in Switzerland. *Atmos. Environ.* **2005**, *39*, 637–651. [[CrossRef](#)]
64. Pateraki, S.; Assimakopoulos, V.; Maggos, T.; Fameli, K.; Kotroni, V.; Vasilakos, C. Particulate matter pollution over a Mediterranean urban area. *Sci. Total Environ.* **2013**, *463–464*, 508–524. [[CrossRef](#)]
65. Khan, M.F.; Shirasuna, Y.; Hirano, K.; Masunaga, S. Characterization of PM_{2.5}, PM_{2.5–10} and PM₁₀ in ambient air, Yokohama, Japan. *Atmos. Res.* **2010**, *96*, 159–172. [[CrossRef](#)]
66. Zhuang, H.; Chan, C.K.; Fang, M.; Wexler, A.S. Formation of nitrate and non-sea-salt sulfate on coarse particles. *Atmos. Environ.* **1999**, *33*, 4223–4233. [[CrossRef](#)]
67. Zhuang, H.; Chan, C.K.; Fang, M.; Wexler, A.S. Size distributions of particulate sulfate, nitrate, and ammonium at a coastal site in Hong Kong. *Atmos. Environ.* **1999**, *33*, 843–853. [[CrossRef](#)]
68. Wioletta, R.-K.; Izabela, S.; Barbara, M.; Krzysztof, K.; Anna, Z.; Kornelia, K. Size-Resolved Water-Soluble Ionic Composition of Ambient Particles in an Urban Area in Southern Poland. *J. Environ. Prot.* **2013**, *4*, 371–379. [[CrossRef](#)]
69. Bauer, S.E.; Koch, D.; Unger, N.; Metzger, S.M.; Shindell, D.T.; Streets, D.G. Nitrate aerosols today and in 2030: A global simulation including aerosols and tropospheric ozone. *Atmos. Chem. Phys.* **2007**, *7*, 5043–5059. [[CrossRef](#)]
70. U.S.EPA. *Atmospheric Ammonia: Sources and Fate: A Review of Ongoing Federal Research and Future Needs*; U.S.EPA: Washington, DC, USA, 2000.
71. Frank, N.H. Retained nitrate, hydrated sulfates, and carbonaceous mass in federal reference method fine particulate matter for six eastern U.S. cities. *J. Air Waste Manag. Assoc.* **2006**, *56*, 500–511. [[CrossRef](#)] [[PubMed](#)]
72. Chow, J.C.; Watson, J.G.; Lowenthal, D.H.; Magliano, K.L. Loss of PM_{2.5} nitrate from filter samples in central California. *J. Air Waste Manag. Assoc.* **2005**, *55*, 1158–1168. [[CrossRef](#)] [[PubMed](#)]
73. Raask, E. The mode of occurrence and concentration of trace elements in coal. *Prog. Energy Combust. Sci.* **1985**, *11*, 97–118. [[CrossRef](#)]
74. Aburas, H.M.; Zytoon, M.A.; Abdulsalam, M.I. Atmospheric Lead in PM_{2.5} after Leaded Gasoline Phase-out in Jeddah City, Saudi Arabia. *Clean-Soil Air Water* **2011**, *39*, 711–719. [[CrossRef](#)]
75. RSC. Royal Society of Chemistry (RSC): Uses and Properties of Lutetium (Lu). Available online: <http://www.rsc.org/periodic-table/element/71/lutetium> (accessed on 6 June 2016).
76. Steinbach, C. Cerium Dioxide (CeO₂)—Overview. nanopartikel.info (2011-02-02). Available online: <http://nanopartikel.info/en/nanoinfo/materials/cerium-dioxide> (accessed on 6 June 2016).
77. Trovarelli, A. *Catalysis by Ceria and Related Materials*; Imperial College Press: London, UK, 2002.
78. Bleiwas, D.I. *Potential for Recovery of Cerium Contained in Automotive Catalytic Converters: U.S. Department of the Interior*; U.S. Geological Survey Open-File Report 2013–1037; U.S. Geological Survey: Reston, VA, USA, 2013; p. 10.